Not peer-reviewed version

Pseudomonas sp. N5.12 Metabolites Formulated in AgNPs Enhance Plant Fitness and Metabolism Without Altering Soil Microbial Communities

Svitlana Plokhovska [*] , Ana García-Villaraco , Jose Antonio Lucas , Francisco Javier Gutiérrez-Mañero ,
Beatriz Ramos-Solano [*]

Article

Pseudomonas sp. N5.12 Metabolites Formulated in AgNPs Enhance Plant Fitness and Metabolism Without Altering Soil Microbial Communities

Svitlana Plokhovska [1,2,*]**, Ana García-Villaraco** [1]**, Jose Antonio Lucas** [1]**, Francisco Javier Gutiérrez-Mañero** [1] **and Beatriz Ramos-Solano** [1,*]

[1] Universidad San Pablo-CEU Universities, Faculty of Pharmacy, Madrid 28668, Spain

[2] Institute of Food Biotechnology and Genomics NAS of Ukraine, Kyiv 04123, Ukraine

* Correspondence: svetaplohovska@gmail.com (S.A.); bramsol@ceu.es (B.R-S.)

Abstract: This study investigates the effects of metabolites from the beneficial bacteria *Pseudomonas* N5.12 formulated as silver nanoparticles (AgNPs) on tomato plants and soil microbial communities, to explore environmental safety of AgNPs for future applications in agriculture. AgNPs coated with bacterial metabolites are endowed with biological activity that is dose dependent, as shown by cytoskeleton alterations in Arabidopsis roots. The results show that N5.12-AgNPs can trigger beneficial effects on tomato plants, either when delivered through the leaves or roots, indicating effectiveness of the metabolites formulated as NP. Effects consist of lowering oxidative stress metabolism and therefore, improving plant resilience, as well as increasing chlorophyll *a* and carotenoid content. The significant reduction of H_2O_2 content was not associated to ROS scavenging enzymes but to an increase in total phenolic content. On the other hand, AgNPs had a minimal impact on bacterial metabolic activity, irrespective of the application way. Microbial communities' structure was not altered by AgNP, anticipating environmental safety for agronomic applications. These findings suggest that *Pseudomonas* N5.12 metabolites formulated in AgNPs, at physiological concentration (30 ppm), may offer agricultural benefits by improving plant health appearing as an environmentally safe alternative for agriculture.

Keywords: silver nanoparticles; toxicity; cytoskeleton; oxidative stress; microbial communities; environmental safety

1. Introduction

Silver nanoparticles have attracted significant interest due to their unique physicochemical properties, including high surface area, ease of functionalization and antibacterial activity. There are different procedures to reduce Ag^+ to Ag^0, from chemical to biological methods resulting in NP synthesis, among which biological synthesis is relevant because it is low cost and environmentally friendly [1]. Biological synthesis procedure will determine size and shape of NP, with a unique organic matter coat that stabilizes NP and modulates effects. Irrespective of their synthesis, NPs are increasingly used in various sectors, including agriculture, medicine, textiles, and electronics [2,3]. As their use in agricultural applications is experiencing great development from pesticides to fertilizers and plant growth stimulants, it is essential to examine their potential impacts on plant physiology and soil ecosystems safety, prior to exploring implications for food security as they may also accumulate on edible parts of the plants [4].

The interaction of AgNPs with plants has been the subject of extensive research, revealing both positive and negative effects on plant growth and development. AgNPs can be absorbed by plant roots and translocated to aerial parts, where they influence various physiological processes, including photosynthesis, nutrient uptake, and stress responses [5]. On one hand, AgNPs enhance seed germination and early-stage growth, likely through improved antioxidant activity and hormonal

signaling [6]; at low concentrations, AgNPs trigger defense mechanisms and ROS production to help plant acclimation [7], increase nutrient absorption [8] and plant growth in different conditions [9,10].

One of the key concerns associated with plant exposure to AgNPs is the potential of these materials to induce oxidative stress, probably due to the release of Ag^+ ions which can bind to plant tissues and disrupt cellular functions. At high concentrations, AgNPs can cause toxicity by inducing oxidative stress, damaging plant cell membranes, and disrupting metabolic pathways [11,12]. In line with this, the cytoskeleton is an excellent marker for this goal since it reacts immediately to environmental stress. Both microtubules and microfilaments disassemble upon stress sensing to repolymerize within a short time if perturbation is not toxic [13]. Hence, alterations of the cytoskeleton structure is a good marker to determine a physiological concentration of AgNPs [14]. Indeed, biologically synthetized AgNP are usually capped and therefore, oxidation of Ag^0 is not likely to occur.

Additionally, recent research has highlighted the potential for AgNPs to influence the soil microbial functional diversity. AgNPs can alter key microbial processes such as carbon and nitrogen cycling, leading to changes in soil quality and the availability of essential nutrients for plants [15]. The impacts on microbial communities may vary depending on soil characteristics (pH, organic matter content) and the form in which silver is applied. AgNPs are known to exert antimicrobial effects, which can lead to shifts in microbial population dynamics that in turn may lead to plant benefits or be detrimental. Several studies have demonstrated that NPs can indirectly promote plant nutrient absorption and ultimately promote plant growth by increasing the richness of rhizosphere microbiota [15,16]. However, AgNPs can inhibit the growth of soil bacteria, fungi, and other microorganisms, potentially disrupting beneficial microbial communities [17]. Thus, while the use of AgNPs in agriculture holds significant promise, it also raises concerns about their potential environmental impact, affecting microbial community structural and functional diversity.

Interestingly, recent studies have reported synthesis of AgNP coated with metabolites from two different beneficial *Pseudomonas* strains able to inhibit microorganisms' growth [18,19]. As *Pseudomonas* strain N5.12 and its metabolites were able to promote plant growth and trigger plant innate immune system [20], we hypothesized that bacterial metabolites formulated in AgNP would trigger plant metabolism without altering rhizosphere microbial communities. As plants determine own rhizosphere microbial communities through exudates, we explored changes after root application to rule out direct inhibitory effect by AgNP, or leaf delivery to rule out indirect systemic effects through exudates. Therefore, this study aims to investigate the effect of *Pseudomonas* N5.12 metabolites formulated as AgNPs on plant growth and soil microbial communities. To achieve these goals, a physiological dose will first be determined based on cytoskeleton disruption in transgenic *Arabidopsis* plants; and secondly, AgNPs will be delivered to tomato plants through leaves or roots, and effects on plant physiology (photosynthetic efficiency, oxidative stress markers and ROS scavenging enzyme activities) and on soil microbial communities' (metabolic and structural diversity) will be studied.

2. Results

2.1. Effect of Biosynthesized AgNPs from Pseudomonas N5.12 on Cytoskeletal Structures in Arabidopsis Roots

This study focused on determining a physiological dose of AgNP by evaluating disruption of cytoskeleton structures. MT orientation varies across root zones, reflecting different stages of cell growth and division. Arrangement of MT in the meristematic zone of native plants, is perpendicular to cell division plane (Figure 1a), while in the elongation zone, they reorganize to a longitudinal orientation to support cell elongation (Figure 1f). In NP treated plants, the epidermal cells of the root elongation zone show MT reorientation 1-hour after treatment with different concentrations of AgNPs. Specifically, after treatment with 30 ppm AgNP, cells exhibit a predominantly longitudinal and oblique orientation (Figure 1b); at 60 ppm, most cells show an oblique arrangement (Figure 1c);

and at 120 ppm, a chaotic MT arrangement predominates (Figure 1d); stock solution (6000 ppm) caused a total disruption of cytoskeleton (data not shown). NPs did not affect MTs length in the elongation zone, which fluctuated within values of control plants (from 18 to 23 μm) across all concentrations studied (Figure 1e). Additional changes in MT organization were observed in root meristematic cells. At a low concentration of AgNP (30 ppm), no significant changes in MT organization were detected, with most of them having a predominantly transverse orientation as in the control (Figure 1g). Higher concentrations of NPs caused disruptions in the structure of MTs, resulting in short filaments randomly distributed throughout the cell cytoplasm (Figure 1h and Figure 1i). In short, MTs length was reduced by 57.7 % and 68.4 % following treatments with NPs at 60 and 120 ppm, respectively (Figure 1k). In summary, AgNP affects the orientation of MTs without dramatic changes in their organization, but higher concentrations shorten MTs.
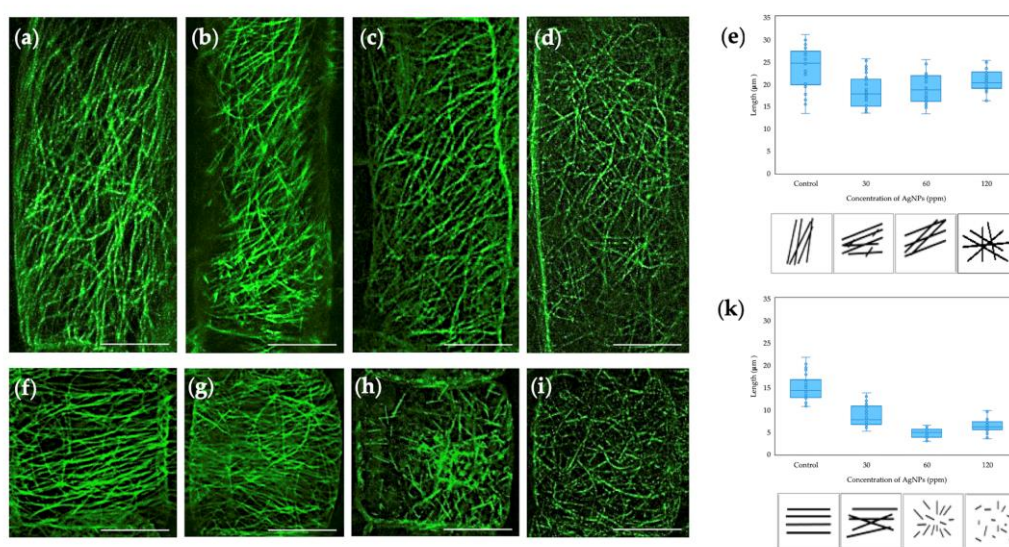

Figure 1. Organization of microtubules in *Arabidopsis gfp-map4* 1 hour after exposure to different AgNP concentrations: control (**a**, **f**); 30 ppm NPs (**b**, **g**); 60 ppm NPs (**c**, **h**); 120 ppm NPs (**d**, **i**). The average size of MTs in the elongation zone (**e**) and meristem (**k**). Epidermal cells of the elongation zone (**a–d**); meristematic cells (**f–i**). The images were taken sequentially with confocal microscopes from Leica Microsystems in the green channel (ex/em: 488/496–556 nm) for GFP visualization. Scale bars: 10 μm.

The effect of AgNP on the structure of Actin Filaments (AFs) in *Arabidopsis* root cells was studied using *gfp-fabd2* mutants. The results revealed that AgNP have a more pronounced impact on AF organization. Elongation cells contain a thin and highly dynamic network of AFs throughout the entire cytoplasm (Figure 2a). When seedlings were exposed to 30 ppm NPs, the AF network thinned somewhat but was like the control (Figure 2b). At higher concentrations, AgNP (60 and 120 ppm) cause AFs to break apart or fragment into shorter segments, disrupting the normal structure and organization of the AF network (Figure 2c and Figure 2d). A similar pattern is observed in meristematic cells, where AgNP causes the disintegration and depolymerization of AFs as the concentration increases from 30 to 120 ppm (Figure 2f–h).

As a result, AgNP disrupt AF length and stability in different root cells. The average size of AFs decreases slightly following treatment with 30 ppm NPs; however, this change remains statistically non significant, as it fluctuates within the range of the control values. In elongating cells, the size of AFs decreased by 77.6 % and 84.8 % following treatment with 60 ppm and 120 ppm NPs, respectively (Figure 2i), indicating a significant disruption in structure at higher concentrations. A similar pattern was observed in the cells of the meristematic zone, where the size of AFs decreased by 67.5 % and 79.8 % (with 60 ppm and 120 ppm NPs, respectively) indicating a concentration-dependent effect on actin structure (Figure 2k).
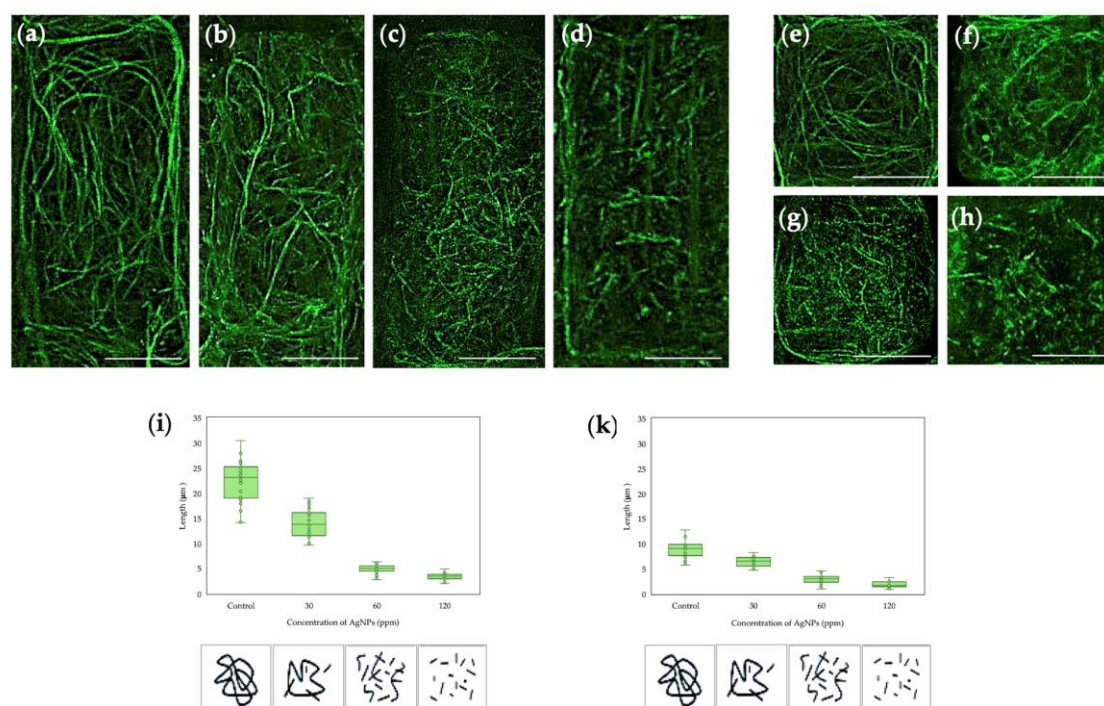
Figure 2. Effect of AgNP on the AFs of *Arabidopsis gfp-fabd2* cells 1 hour after treatment: control (**a**, **e**); 30 ppm NPs (**b**, **f**); 60 ppm NPs (**c**, **g**); 120 ppm NPs (**d**, **h**). The average size of AFs in the elongation zone (**i**) and meristem (**k**). Epidermal cells of the elongation zone (**a**–**d**); meristematic cells (**e**–**h**). The images were taken sequentially with confocal microscopes from Leica Microsystems in the green channel (ex/em: 488/496–556 nm) for GFP visualization. Scale bars: 10 μm.

Therefore, low concentrations of AgNP are less likely to cause significant toxicity or major disruption of cytoskeleton dynamics in *Arabidopsis* roots. Based on these data, a concentration of 30 ppm AgNPs was selected for further research on plants growth and development.

2.2. Biological Effects of AgNPs on Tomato Plants

The effect of AgNP from *Pseudomonas* N5.12 in tomato was studied, measuring photosynthetic performance and pigments. When photosynthetic efficiency was evaluated, non-significant differences were found in any parameter, although non photochemical quenching (NPQ) showed a notable non-significant increase (Supplementary Figure S1). NPs positively affected the level of photosynthetic pigments, irrespective of the delivery way. Root treatment resulted in 14.2 % increase in chlorophyll *a* content, while the leaf treatment led to a significant increase by 25.2 % (Figure 3a); however, chlorophyll *b* content did not show any significant variation compared to the control (Figure 3b). More notable changes were observed in carotenoid content, which increased by 36 % and 46.6 % following root and leaf treatments, respectively (Figure 3c). Silver nitrate did not affect photosynthetic pigments concentration.
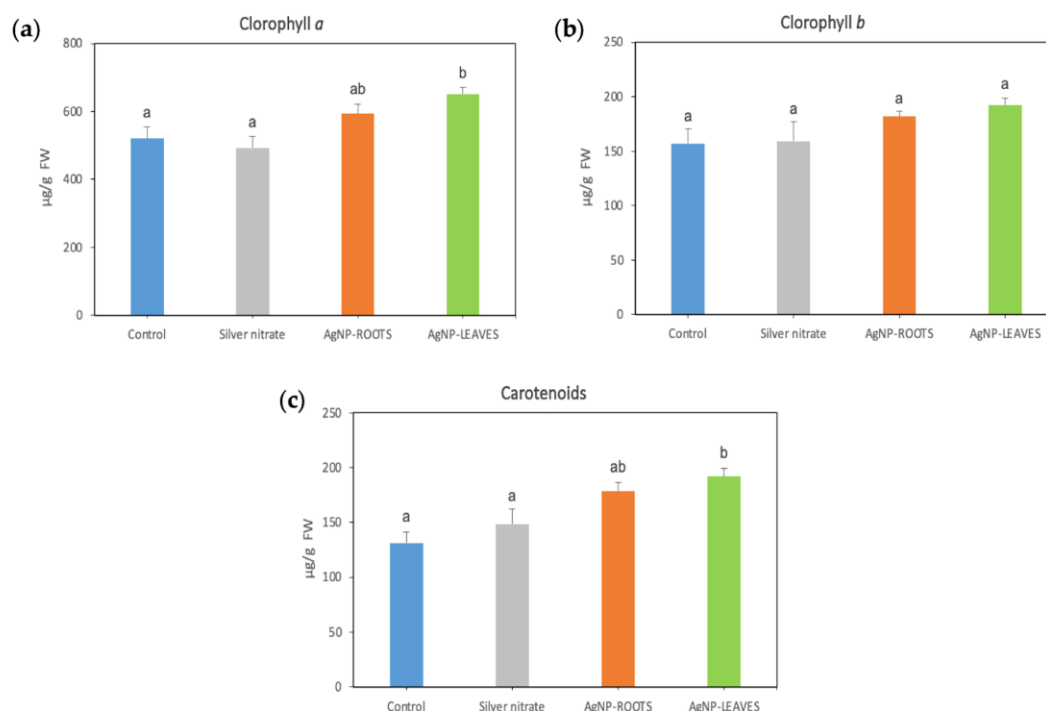
Figure 3. Photosynthetic pigments concentration (units) in 7-week-old tomato plants: chlorophyll *a* (**a**); chlorophyll *b* (**b**) and carotenoids (**c**). Values are recorded as mean ± standard error of a triplicate experiment. Different letters indicate significant differences according to ANOVA and LSD post hoc test (p < 0.05).

A significant decrease in the content of H_2O_2 by almost 3 times was observed in both root and leaf treated plants. In contrast, when treated with 1 mM $AgNO_3$, the H_2O_2 content increased by 1.3 times compared to the control (Figure 4a), MDA content was similarly enhanced by all treatments (Figure 4b). At the same time, the activity of the ROS scavenging enzymes APX and CAT under AgNP treatments were not statistically different from those of the control plants (Figures 5a and 5b). However, exposure to NPs significantly increased the total phenolic content in tomato plants, with the highest values observed in leaf-treated plants (1.588 mg/g FW) compared to the control and similar to silver nitrate (Figure 6).
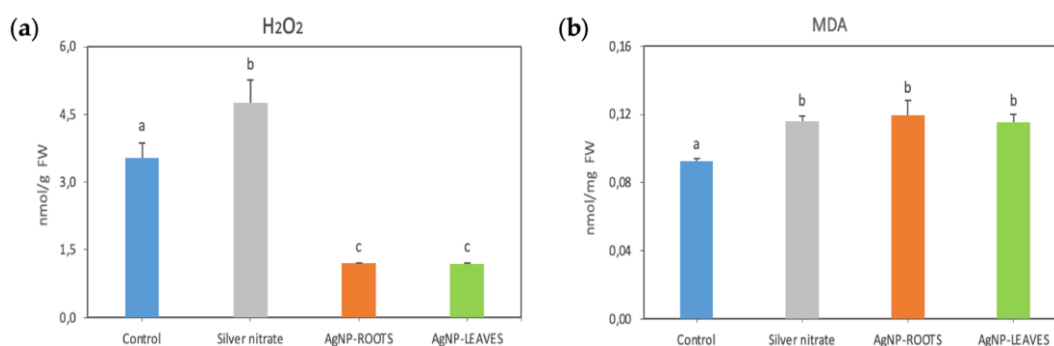

Figure 4. Oxidative stress markers (units): hydrogen peroxide (**a**) and malondialdehyde (**b**) in 7-week-old tomato plants. Values are recorded as mean ± standard error of a triplicate experiment. Different letters indicate significant differences according to ANOVA and LSD post hoc test (p < 0.05).

Figure 5. ROS Scavenging enzymes activity (units): ascorbate peroxidase (**a**) and catalase (**b**) in 7-week-old tomato plants. Values are recorded as mean ± standard error of a triplicate experiment. Different letters indicate significant differences according to ANOVA and LSD post hoc test ($p < 0.05$).
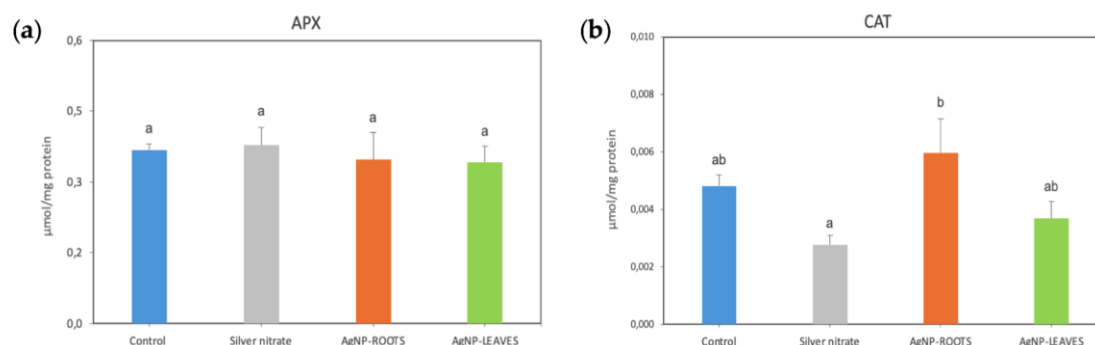

Figure 6. Total phenolic compounds (units) in 7-week-old tomato plants. Values are recorded as mean ± standard error of a triplicate experiment. Different letters indicate significant differences according to ANOVA and LSD post hoc test ($p < 0.05$).
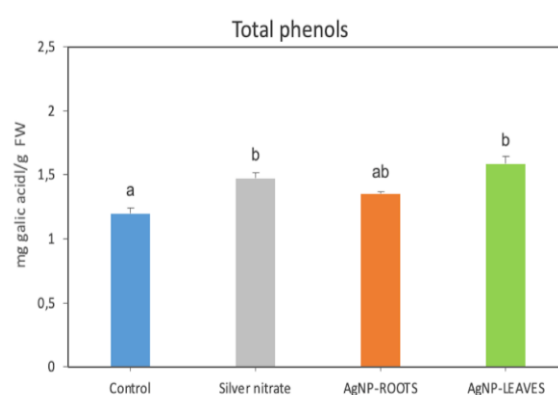
3.3. Microbial Community Diversity and Composition

The average well color development (AWCD) reflects the overall metabolic activity of rhizosphere bacterial community. Kinetics of AWCD are shown in Figure 7a. To further investigate how AgNPs alter the metabolic profile of soil microorganisms, 31 carbon sources utilization was analyzed. The heat map and metabolic profile performed with the absorbance values of the different carbon sources of Biolog Eco plates are presented in Figure 7b and Figure 7c, respectively. Metabolic fingerprint showed in the heat map is similar among all treatments, being the treatment with $AgNO_3$ the one with slight differences in the use intensity of few wells compared with the control (α-cyclodextrin, L-arginine, L-threonine, Putrescine). The use intensity of polymers, carbohydrates, carboxylic acids, amino acids, amines, and phenolic compounds by rhizosphere bacteria was not altered by any treatment (Figure 7c). The metabolic profile was significantly different only between $AgNO_3$ and Control (Figure 7c). Metabolic diversity calculated as Shannon index did not indicate significant differences between treatments (Control: 4.808 ± 0.023; Silver: 4.761 ± 0.017; NP-roots: 4.777 ± 0.019; NP-leaves: 4.722 ± 0.066).
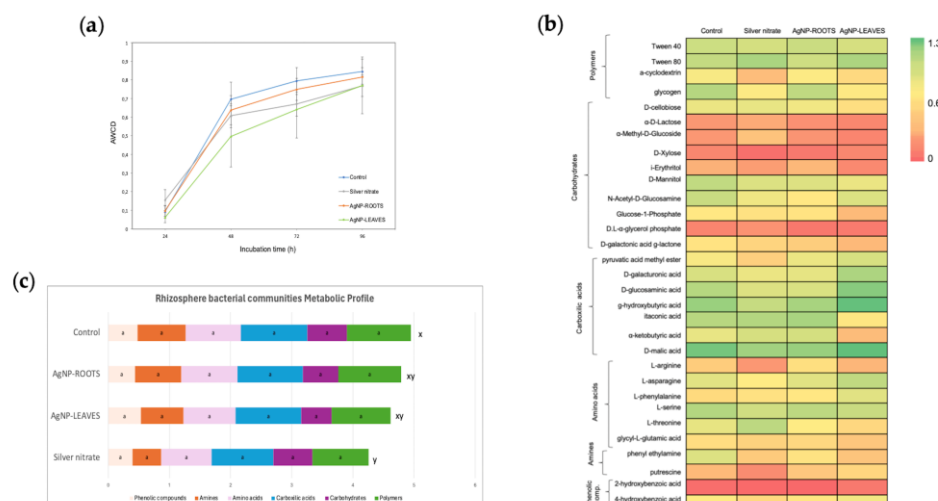
Figure 7. Metabolic activity of rhizosphere bacterial community. (**a**) Average well color development (AWCD) in Biolog Eco plate on 96 hours incubation performed as the mean of the absorbance value of the 31 wells of Biolog Eco plate; (**b**) Heat map performed with the absorbance values of the 31 wells of Biolog Eco plate, measured at 96 hours of incubation; (**c**) Metabolic profile of bacterial communities displayed as bars graph with the mean absorbance values of the substrates of each category (polymers, carbohydrates, carboxylic acids, amino acids, amines and phenolic compounds). Different letters indicate statistically significant differences between treatments (x, y, z) or categories (a, b, c) according to ANOVA and LSD post hoc test ($p < 0.05$).

Structural diversity of rhizosphere microbial communities under the different treatments was analyzed. Biological diversity (Shannon-Weaver index) and abundance were calculated, both for bacterial and fungal communities. The Shannon index for bacteria showed no significant changes between treatments, suggesting that bacterial diversity remained stable under AgNP treatments (Figure 8a). The Shannon index for fungi was similar for controls and both NP treatments; however, significantly lower values were found for the $AgNO_3$ treatment (Figure 8b).

EasyMap did not found significant differences in any taxonomic level between treatments. It is remarkable that the most abundant bacteria phyla were Proteobacteria, Bacteroidetes, Planctomycetes, Acidobacteria and Verrucomicrobia, which dominated more than 84 % of the total sequences (Figure 8c). The relative abundance of Proteobacteria was highest in all samples and remained stable after NP treatment, showing an increase of 4–5.5 %. In contrast, after $AgNO_3$ treatment, the abundance of Proteobacteria decreased by 7.06 % compared to the control. A similar pattern was observed for other bacteria phyla, indicating a possible negative effect of $AgNO_3$ on this microbial group. Thus, AgNP did not alter microbial communities, with no significant changes in microbial structural or metabolic diversity.
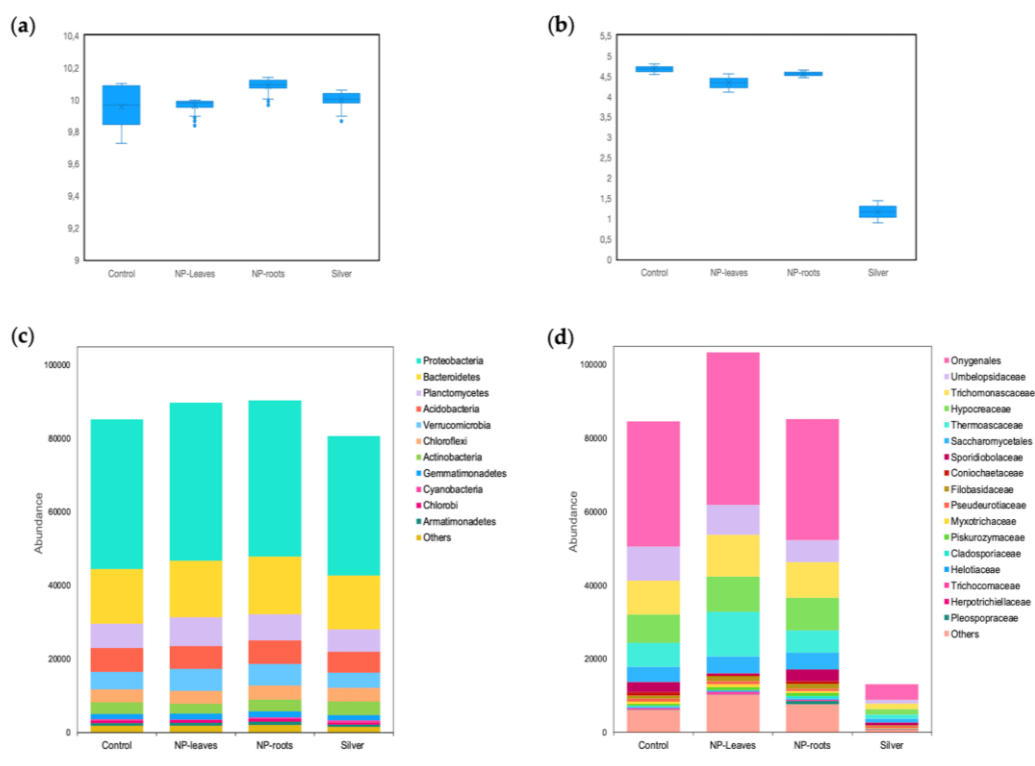
Figure 8. Differences in the structural diversity of bacterial and fungal communities under different AgNP treatments. Biological diversity calculated with Shannon-Weaver diversity index of bacteria (**a**) and fungi (**b**); and the relative abundance of bacterial community at Phylum level (**c**) and fungal community at Family level (**d**).

The fungal community predominantly comprised Onygenales, Umbelopsidaceae, Trichomonascaceae, Hypocreaceae, Thermoascaceae and Saccharomycetales, which accounted for more than 83 % of all fungi (Figure 8d). While AgNP treatments enriched the relative abundance of Onygenales by 3.2 % and 22.1 % after NP-roots and NP-leaves treatments, respectively, as well as the relative abundance of Trichomonascaceae and Hypocreaceae by 6.9 % and 12.6 % (NP-roots), and by 24.2 % and 22.3 % (NP-leaves), respectively. However, AgNP treatments reduced the relative abundance of Umbellopsidaceae by 36.4 % (NP-roots) and 12.8 % (NP-leaves). It is interesting that the relative abundance of Thermoascaceae increased by 90.8 % in the NP-leaf treatment, but it showed only a slightly difference compared to the control in the NP-root treatment. In addition, AgNO$_3$ caused a significant alteration on the fungal community with the relative abundance of all fungal families decreasing by more than 85 %.

3. Discussion

The use of AgNP in agriculture is on the rise and still, evidence for environmental and health safety need to be provided. In a previous work, the process for biological synthesis of AgNP coated with metabolites from the PGPR strain *Pseudomonas* sp. N5.12 was reported, together with the antimicrobial and antifungal effects of these AgNP [18]. As plant protection effects against pathogens and drought have been reported [20,21], a similar or even better effect of the NP is foreseen. As a first step towards this goal, the present study was conceived to explore potential negative effects on soil microbial communities or in plants in order to provide preliminary evidence of their ability to trigger plant metabolism and for environmental safety. Results show that AgNP can trigger plant metabolism without altering microbial communities' structure and activity.

Determining biological activity calls for sensitive and suitable markers. The cytoskeleton is an excellent marker for this goal, since it reacts immediately to environmental stress since both microtubules and microfilaments disassemble upon stress sensing to repolymerize within a short

time if perturbation is not toxic [14]. AgNP can significantly impact the organization and function of MTs and AFs, as metal NPs may lead to damage to the plant's cellular structures in the event of NP uncapping or Ag oxidation, since silver itself is ten times denser than the cytosol. The exact effects depend on various factors, including the size, shape, concentration, and surface properties of the nanoparticles, as well as the exposure duration [13]. Previous studies have shown that exposure to AgNPs leads to a significant reduction in the number and growth rate of MTs in *Arabidopsis* plants [14]. Some studies have shown that AgNPs might induce bundling or aggregation of microtubules, which can alter the typical parallel arrangement of microtubules in plant cells [14,22]. In the case of AgNP, the crown of bacterial metabolites stabilizes and caps the metal, preventing or eliminating toxicity, as evidenced by the non-significant changes on cytoskeleton arrangements by the lower concentration. Consistently, higher concentrations led to MT and AF shortening suggesting a physical interference when NP are too concentrated, as AgNPs can disrupt MTs and AFs organization (Figures 1 and 2) by inhibiting polymerization and leading to the depolymerization or the formation of unstable structures. This study highlights the concentration-dependent toxicity of AgNPs and their potential to interfere with crucial cellular processes, such as cell division and elongation. So based on cytoskeleton response, a physiological active concentration has been established in *Arabidopsis* using *gfp-map4* and *gfp-fabd2* mutants.

Nanoparticles smaller than 60 nm are ideal for penetrating plant tissues because they can navigate stomata (10–60 μm) and plasmodesmata (20–50 nm) [23]. Their shape also influences their entry efficiency, with spherical nanoparticles being the most effective. Spherical AgNPs typically demonstrate better penetration and distribution within plant tissues compared to irregularly shaped particles. Once inside, they can be transported through vascular tissues to deliver nutrients, pesticides, or antimicrobial agents [24]. As the size of our AgNP (average diameter of 20 nm) allows penetration through plant tissues, and tissues are similar in all plant species, we reasoned that the same concentration would suit tomato plants. Furthermore, as AgNP are prone for systemic transport due to size, two application systems were explored, considering effects on soil rhizosphere communities from both ends, directly in the roots, or as a side effect from systemic transport within the plant or by dripping from leaves.

A number of beneficial effects of biologically synthetized AgNP from seed germination to plant growth stimulation have been reported [8,25]. Improving nutrient contents, maintaining the structural integrity of chloroplasts and other cellular components involved in photosynthesis or enhancing pigment synthesis in plants have also been described as mechanisms to improve plant fitness [26]. Although our AgNP did not affect chlorophyll fluorescence, the total chlorophyll and carotenoid content significantly increased, consistent with other authors [27,28]. Interestingly both treatments triggered tomato plants, with leaf treatments having a more pronounced effect than root treatment, evidencing both a systemic effect from the roots, and a direct effect when delivered on the leaf.

In line with improvement of plant fitness, oxidative stress response has been studied. Reactive oxygen species (ROS) increase upon exposure to AgNP, being ROS alteration a general plant response to integrate environmental changes. ROS changes can have different effects depending on their concentration; while high ROS levels may damage tissues, low levels can trigger beneficial responses [29]. Upon stimuli, the plant systems initiate a framework for scavenging ROS by upregulating the activities of antioxidant enzymes, as well as the antioxidants phenols and flavonoids to restore physiological homeostasis [7]. The ability of AgNPs to enhance the activity of ROS scavenging enzymes enhancing the plants' ability to resist oxidative stress and maintain cellular homeostasis under stressful conditions has been reported [29,30]. Our results are consistent with improving ROS homeostasis as indicated by the significant decrease (66%) in H_2O_2 content detected (Figure 4a); this ROS control is based on antioxidant molecules like phenols instead of ROS scavenging enzymes activities (Figures 5 and 6). In line with lower H_2O_2 concentration indicative of non-stressing conditions, lower MDA levels were expected; however, an unexpected 29% increase in MDA content for both root and leaf treatment were found (Figure 4b), suggesting that MDA could be acting as a

signaling molecule [31] in view of the improved physiological status of plants. The protective effects of bacterial metabolites on the NP's crown is evidenced on the different response shown by the increase in H_2O_2 levels compared to the control and to treatment with 1 mM $AgNO_3$.

Environmental safety of the AgNP was the second concern addressed in this work, since our AgNP have demonstrated antimicrobial activity of AgNP against human and plant pathogens [18]. Microorganisms play a key role in soil fertility and are vital for supporting the functions of soil ecosystems. However, the presence of contaminants can interfere with these functions, including the cycling of nitrogen [32]. NPs participate in various physical, chemical, and biological processes, including vulcanization, flocculation, precipitation, and adsorption. These processes allow them to interact with soil organic matter, plants, and microorganisms in the soil [15]. NPs can impact rhizospheric microorganisms positively or negatively, depending on their size, concentration, soil type, and microbial diversity in the root zone [33]. Monitoring rhizosphere bacteria overall metabolic activity (kinetics of AWCD) can provide insights into how AgNPs affect microbial ecosystems. In the literature, soil extract exposures (ex-situ) to uncoated AgNPs and ionic silver resulted in decreases in bacterial metabolic activity [34,35]. However, our data supports the non-toxic effects of our coated NP as either treatment had a minimal impact on functionality of bacterial communities (Figure 7), consistent with functional diversity calculated applying the Shannon-Weaver index. However, when analyzing the metabolic profile (Figure 7c) a significant negative overall effect of $AgNO_3$ was detected, although no significant differences were found when analyzing consumption by compound categories. This indicates that AgNPs functionalized with the metabolites released by N5.12 to the culture medium efficiently reduces silver to form the NP and stabilizes it, preventing oxidation of Ag, and therefore, avoiding the potential negative impact of oxidized Ag on the metabolic activity of rhizobacteria. All this suggests that, at the concentrations used in our study, AgNPs may have limited ecological consequences for soil microbial communities' function.

Nevertheless, despite the overall metabolic activity seems to remain stable, the community composition could shift, with more resistant species dominating the environment. Metagenomic analysis have evidenced changes in specific groups upon NP treatment; among these groups abundance of Acidobacteria, Verrucomicrobia, Actinobacteria, Cyanobacteria and Nitrospirae has been negatively affected by NP, while Proteobacteria and Bacteroidetes abundance increased under NP treatments [17,36]. Proteobacteria have already been identified in other studies as the most prevalent bacterial group in the rhizosphere [37,38]; among other reasons, due to their decisive role in the nitrogen cycle [39]. Our data is consistent with reported effects of NP in this group, showing a similar increase in Proteobacteria abundance by root and leaf treatments, reinforcing the notion of effectiveness of NP both on a direct basis when root treatment is delivered, and by a systemic effect on leaf treatments. Interestingly, stability of the coated NP is also confirmed for microbial communities' structure, as Ag in its ionic form significantly decreased Proteobacteria abundance.

As regards to fungal structure, AgNP have shown to increase prevalent fungal communities, having a slight negative effect only on Umbelopsidaceae. Leaf application seems to affect fungal communities more intensely than root applications, suggesting intense metabolic changes in plants to be responsible for these changes. Finally, toxicity of $AgNO_3$ was confirmed by significant reduction in fungal family abundance by more than 85%, indicating a strong inhibitory effect (Figure 8). These findings support the notion that the form of silver (NPs versus ionic) plays a crucial role in shaping microbial and fungal community composition, with AgNPs generally exerting a more stable and less toxic effect compared to their ionic counterparts [35], confirming the stabilization of the metal due to the corona of bacterial organic matter and its beneficial effects as anticipated in our hypothesis based on the beneficial effect of the strain and its rhizosphere origin.

4. Materials and Methods

4.1. Biosynthesis of AgNP from Pseudomonas N5.12

AgNP were obtained as described in Plokhovska et al. [18]. In summary, 24 h cell free supernatants were mixed with 1 mM AgNO$_3$ (2:4; v/v) and incubated at 37 °C for 24 h. After washing, the product was lyophilized and resuspended in 1 mL of milli Q water with a stock concentration of 6000 µg/mL. It was confirmed by UV-Vis spectra (430 nm) and TEM showing spherical particles (20.71 ± 0.43 nm) with an organic corona of bacterial metabolites (Supplementary Figure S2).

4.2. Determination of Physiological Dose in Transgenic Arabidopsis

The experiments were performed using 5-day-old seedlings of the *Arabidopsis thaliana* plants (GFP-MAP4 and GFP-FABD2) with fluorescently labeled microtubules and actin filaments, respectively. The mutant lines were obtained from the European Arabidopsis Stock Centre (NASC; https://arabidopsis.info), stock codes N799990 and N73159. *Arabidopsis* seeds were sterilized in 70% EtOH (1.5 min) and 10% sodium hypochlorite (10 min) and exposed to cold stratification for 2 days. After stratification, the seeds were sown on agar plates under sterile conditions. Seedlings were grown in a vertical position in a climate chamber (Sanyo MLR-350H) at 22 °C, 70% air humidity, under long day conditions (12 h light period). Five-day-old seedlings were transferred for 1 hour to different concentrations of AgNPs (30, 60 and 120 ppm) to study their effect on the plant cytoskeleton. Changes in the organization of MTs and AFs in the cells of the elongation zone and root meristem were observed using a Leica Stellaris 8 Confocal Microscopy (SAI-MICROCON), https://www.uspceu.com/en/research/research-support/servicio/microsco pia-confocal. The fluorescent signal from GFP was excited at 488 nm and emitted at 505/530 nm. To measure the lengths of MTs and AFs ImageJ software (Version 1.8.0_345) was used. The measurements were carried out on confocal microscope images specifically within the elongation zone and meristematic cells (n = 30).

4.3. Experimental Design: Effect of AgNPs on Tomato Plants and Microbial Communities

Experiments were conducted to investigate if the physiological dose of AgNPs in *Arabidopsis* was effective in tomato plants *Lycopersicon esculentum* Razymo RZ (F1-Hybrid 74-204RZ), and to explore changes in rhizosphere microbial communities. Two ways to deliver AgNP were evaluated: leaf spray or root drench.

Experimental design is shown in Figure 9. Seeds were sown in trays (4) of 12 alveoli. Each tray was watered with 1 L of tap water every two days and were grown in the greenhouse, under natural photoperiod, with a day-night temperature range of 10 °C to 30 °C. One month after sowing, 24 seedlings (two trays) were inoculated with AgNPs, 12 seedlings (one tray) were inoculated with 1 mM AgNO$_3$, leaving 12 seedlings (1 tray) as control. Treatment with AgNPs (30 µg/mL) were delivered to the leaves adding a drop on the newest leaf (50 µL/plant; one tray) or inoculated by soil drench (5 mL/plant; one tray). Treatments were delivered 3 times, with 3 days between each application; fist application was done on 4-week-old tomato plants (Figure 9). Four days after the last treatment, the plant's aerial parts were harvested, powdered in liquid nitrogen, and stored at -80°C. Rhizosphere soil was sampled and stored -80º until further analysis. The 12 plants per treatment were sampled, and material from 4 plants was pooled and constituted a replicate.
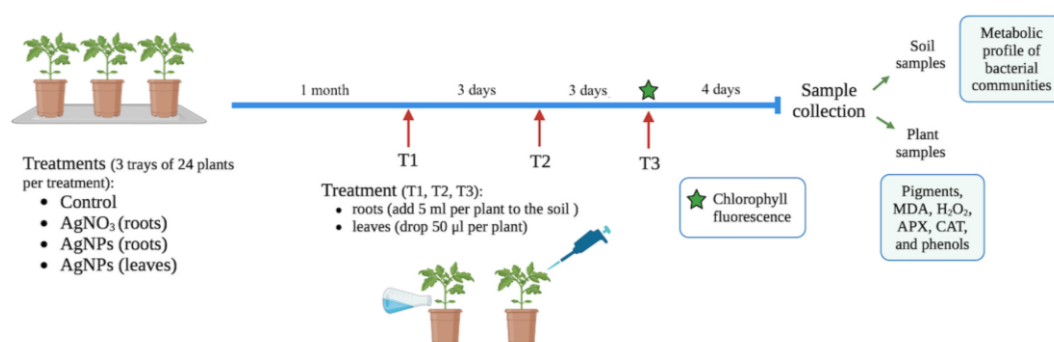
Figure 9. Experimental design.

4.4. Effects on Plant Physiology

4.4.1. Chlorophyll Fluorescence

Photosynthetic efficiency was assessed based on the chlorophyll fluorescence emitted by photosystem II. Chlorophyll fluorescence was measured with a pulse amplitude modulated (PAM) fluorometer (HansatechFM2, Hansatech, Inc., UK) on 1 h dark-adapted leaves. The variable fluorescence (Fv) was calculated as the difference between the maximum fluorescence (Fm) and the minimum fluorescence (Fo). The maximum photosynthetic efficiency of photosystem II (PSII) was calculated as Fv/Fm. Immediately, the leaf was continuously irradiated with red-blue actinic beams and equilibrated to record steady-state fluorescence signal (Fs). The effective PSII (φPSII) and non-photochemical quenching coefficient (NPQ) were calculated as follows: φPSII = (Fm'-Fs)/Fm') and NPQ = (Fm-Fm')/Fm'). All measurements were carried out in the five plants of each treatment [20].

4.4.2. Photosynthetic Pigments

One hundred milligram of leaf powder was dissolved in 1 mL of acetone 80 % (v/v), incubated overnight at 4 °C, and then centrifuged 5 min at 10,000 rpm in a Hermle Z233 M-2 centrifuge. Absorbance at 647, 663, and 470 nm was measured immediately to quantify chlorophyll *a*, chlorophyll *b*, and carotenoids using a Biomate 5 spectrophotometer. Concentration of chlorophylls *a* and *b* was calculated with the equations proposed by Porra et al. [40] and carotenoids with the one proposed by Lichtenthaler [41].

Chl a (μg/g FW) = [(12.25×Abs663) − (2.55×Abs647)] × V(mL)/weight (g).

Chl b (μg/g FW) = [(20.31×Abs647) − (4.91×Abs663)] × V(mL)/weight (g).

Carotenoids (μg/g FW) = [(1000×Abs470) − (1.82×Chl a) − (85.02×Chl b)/198] × V(mL)/weight (mg).

4.4.3. Oxidative Stress Markers

The quantification of H_2O_2 was performed following the method shown in Shukla et al. [42]. Samples (0.2 g) were suspended, and vortexed with 2.0 mL of 0.1% (w/v) trichloroacetic acid (TCA) in an ice bath. The homogenate was centrifuged at 10,000× g for 20 min. The supernatant (0.5 mL) was mixed with 0.5 mL of 10 mM of potassium phosphate buffer (pH 7.0) and 1 mL of 1 M potassium iodide. After 5 min, absorbance was measured spectrophotometrically at 390 nm. The amount of H_2O_2 formed was estimated from a standard curve and expressed as nmol/g H_2O_2 of FW.

Malondialdehyde (MDA) content was determined as described by Hu et al. [43]. Briefly, 0.1 g of powder was added to 2 mL of 10% (v/v) trichloroacetic acid (TCA) and centrifuged at 20,000× g for 30 min at 4 °C. The supernatant (1 mL) was mixed with 4 ml TCA 20 % with thiobarbituric acid (TBA) 0.5 % (v/v). The supernatant (1 mL) was mixed with 4 mL of 20 % TCA and 0.5 % thiobarbituric acid (TBA). The reaction was incubated at 95 °C for 30 min and cooling to room temperature. Then, it was

centrifuged at 10,000× g for 10 min and the absorbance at 532 and 600 nm of the supernatant was measured. The concentration of MDA was determined as: MDA (nmol/g FW) = [(Abs 532 − Abs 600)]/(ε × FW), where ε is the molar extinction coefficient (155 mM$^{-1/cm}$).

4.4.4. Enzyme Activities

To determine enzyme activity a buffered enzyme extract was prepared (10 mg of leaf powder in 1 mL of potassium phosphate buffer 0.1 M pH 7 supplemented with 2 mM Phenylmethyl sulfonyl fluoride), manipulated at 4 °C. After 10 min of sonication, followed by centrifugation (10 min) at 14,000 rpm, soluble proteins were determined in the supernatant. Then, 50 µL of supernatant were mixed with 250 µL of Bradford reagent to determine total protein on ELISA 96-well plates. After 30 min at room temperature, absorbance at 595 nm was determined in a plate reader (Heales MB-580). A calibration curve was constructed from commercial BSA (0.05 and 2 mg/mL) to interpolate absorbances and determine protein concentration. Enzyme activities related to scavenging of ROS were determined in the supernatant with a spectrophotometer.

Ascorbate peroxidase (APX) was measured by the method as shown in García-Limones et al. [44]. The enzyme extract (100 µL) was mixed with 860 µL of potassium phosphate buffer (50 mM pH 7.0) and 120 µL of 2.5 mM sodium ascorbate. The reaction was started by adding 120 µL of 50 mM H_2O_2. A decrease in absorbance at 290 nm was indicative of the oxidation of ascorbate. Activity was calculated using the extinction coefficient of 2.8 mM$^{-1/cm}$.

Catalase (CAT) was measured by the method in García-Limones et al. [44]. The enzyme extract (50 µL) was mixed with 980 µL of potassium phosphate buffer (50 mM pH 7.0) and 120 µL of 200 mM H_2O_2. The absorption at 240 nm was measured immediately and after 20 seconds; a decrease indicates H_2O_2 breakdown. Activity was calculated using the extinction coefficient of 36 mM$^{-1/cm}$.

4.4.5. Total Phenols

Total phenols were quantitatively determined with Folin–Ciocalteu agent (Sigma Aldrich, St Louis, US) by a colorimetric method with some modifications [45]. Twenty microliters of extract were mixed with 250 µL of Folin-Ciocalteu agent, 750 µL of Na_2CO_3 20 % solution and 950 µL H_2O. After 2 hours at room temperature, absorbance was measured at 760 nm. A gallic acid calibration curve was made (r = 0.99). Results are expressed in mg of gallic acid equivalents per 100 g of FW.

4.5. Effects on Microbial Communities

4.5.1. Metabolic Profile of Soil Microbiota

Biolog® ECO plate (BIOLOG Inc., Hayward, CA) were used to assess metabolic profile and diversity 8 of the bacterial communities [46]. Biolog ECO plates are 96-well microplates that contain 31 substrates in triplicate (providing three repetitions per replicate, 3 replicates; n=9) and three control wells without a substrate.

A bacterial suspension was prepared homogenizing 2 g of rhizosphere soil in 20 ml of sterile distilled water by stirring for 15 min. The homogenate was centrifuged for 10 min at 2,500 rpm and the supernatant was filtered through glass wool. The bacterial suspension obtained was resuspended in $MgSO_4$ 10 mM to achieve 95 % of transmittance at 620 nm. The wells of the plate were inoculated with 150 µl per well of this bacteria suspension. Plates were incubated at 25 °C in darkness and the absorbance at 595 nm of the wells was measured every 24 h until 96 h with a HEALES "MB-580" ultrafast automatic microplate reader. Each absorbance value was corrected by subtracting the blank (corrected absorbance).

The corrected mean absorbance of all wells, known as average well color development (AWCD) was calculated and plotted against incubation time to obtain growth curves of the microbial community in the wells of the plate. In these curves, the incubation time was chosen at which the growth of the microorganisms was starting the stationary phase, which was 96 hours. With the

corrected absorbance values of the chosen incubation time (96 h), the metabolic diversity of each sample was calculated using the Shannon-Weaver diversity index [47]:

H = - S [ni/N * Log ni/N],

where: ni = Corrected absorbance of each substrate (well); N = Sum of the 31 corrected absorbance values.

4.5.2. Metagenomic Analyses of the Rhizosphere Bacterial and Fungi Communities

Metagenomic analyses were carried out by AllGenetics & Biology SL (www.allgenetics.eu). DNA was extracted from 250 mg of each rhizosphere sample using the DNeasy PowerSoil Pro kit (Qiagen) following the manufacturer's instructions, with an extraction blank (Bex) included to check for contamination. The DNA was resuspended in 50 µL and quantified using the Qubit High Sensitivity dsDNA Assay (Thermo Fisher Scientific).

For the rhizosphere bacterial community library preparation, the 16S rRNA gene (domains V4-V5, around 400 bp) was amplified using the following primers: forward 515F-Y (5'-GTGYCAGCMGCCGCGGTAA-3') [48] and reverse 926R (5'-CCGYCAATTYMTTTRAGTTT-3') [49].

For rhizosphere fungi community library preparation, a fragment of the ITS1 genomic region (of around 300 bp) was amplified using the following primers: Forward ITS1F (5' CTTGGTCATTTAGAGGAAGTAA 3') [50] and reverse ITS2 (5' GCTGCGTTCTTCATCGATGC 3') [51]. In both libraries the pool was sequenced in a fraction (1/16) of a MiSeq PE300 flow cell (Illumina).

EasyMAP, a user-friendly online platform for evaluating 16S rRNA sequencing data was utilized [52]. For alpha diversity analysis, EasyMAP produces "observed OTUs", "Faith's Phylogenetic Diversity", "Shannon index", and "Pielou's evenness". Microbes with significant differences across groups are identified using LEfSe, which EasyMAP applies to provide taxonomic differential abundance analysis. When conducting a Wilcoxon test between distinct subgroups, the default alpha value is 0.05. Two is the standard threshold for the logarithmic linear discriminant analysis (LDA) score's absolute value. For the Kruskal–Wallis test between statistical groups, the default alpha value is 0.05. Finally, the Greengenes database (version 13_8, 99% OTU) and VSEARCH [53] are used for close-reference clustering to predict the function of the microbes. This ensures that the representative sequences map to the Greengenes database. PICRUSt locates the matching function in the KEGG database using the mapped Greengenes ID.

For fungi, taxonomic assignment of each ASV (Amplicon Sequence Variant) was performes using a pre-trained classifer of the UNITE reference database [54]; updated in May 2021. Specifically, the feature-classifier approach classify-sklearn implemented in QIIME 2 [55], setting the confidence parameter at 0.80 was used.

4.6. Statistics

To examine the statistical differences in the stem diameter and height between treatments in each sample period (June 19 and June 20), one-way ANOVA with repetitions was carried out. IBM SPSS Statistics (Version 29.0.2.0) was used to verify the homoscedasticity and normality of the variance prior to ANOVA analysis, ensuring that all the analytical conditions were met. LSD test was employed when significant differences ($p < 0.05$) were observed. The sequences obtained in the metagenomic analysis were analyzed using an online platform for analyzing 16S ribosomal DNA sequencing data named EasyMAP [54]; accessed on December 10, 2020.

5. Conclusions

In summary, the following conclusions can be made:

- The metabolites from *Pseudomonas* N5.12 formulated in AgNPs have biological activity that is dose dependent, as shown by cytoskeleton alterations.

- Physiologically active doses are low and can be extrapolated to different plant species. AgNP coated with N5.12 metabolites (N5.12-AgNP) can effectively enhance tomato metabolism,

highlighting the potential of nanotechnology-based solutions to promote sustainable agriculture.

- N5.12-AgNPs enhance plant resilience on tomato plants. Despite the increase in photosynthetic pigment contents and in MDA, H_2O_2 levels decreased, suggesting that coated AgNPs contribute to oxidative stress homeostasis in plant cells, modulating antioxidant molecules for ROS scavenging without involving major changes in specific antioxidant enzymes.

- N5.12-AgNPs did not significantly affect overall microbial diversity or activity, anticipating environmental safety. Furthermore, NP treatments favored beneficial bacteria groups like Proteobacteria.

- N5.12-AgNP can be delivered to the roots or to the leaves achieving similar effects either directly or systemically. Further studies are necessary to unveil differences.

- When formulated in AgNP, N5.12 metabolites are able to reduce silver, stabilizing the NP and preventing negative effects that could arise from oxidation of silver after delivery; negative effects have been evidenced on $AgNO_3$ treatments at all levels.

- N5.12-AgNPs enhance plant fitness while maintaining rhizosphere microbial balance.

Conflicts of Interest: The authors declare no conflicts of interest.

Abbreviations

The following abbreviations are used in this manuscript:

AgNP	Silver nanoparticles
MT	Microtubules
AF	Actin Filaments
APX	Ascorbate peroxidase
CAT	Catalase
MDA	Malondialdehyde
H_2O_2	Hydrogen peroxide
AWCD	Average Well Color Development

References

1. Dhaka, A.; Chand Mali, S.; Sharma, S.; Trivedi, R. A review on biological synthesis of silver nanoparticles and their potential applications. *Results Chem.* **2023**, *6*, 101108. https://doi.org/10.1016/j.rechem.2023.101108

2. Nie, P.; Zhao, Y.; Xu, H. Synthesis, applications, toxicity and toxicity mechanisms of silver nanoparticles: A review. *Ecotoxicol. Environ. Saf.* **2023**, *253*, 114636. https://doi.org/10.1016/j.ecoenv.2023.114636

3. Mgadi, K.; Ndaba, B.; Roopnarain, A.; Rama, H.; Adeleke, R. Nanoparticle applications in agriculture: overview and response of plant-associated microorganisms. *Front. Microbiol.* **2024**, 15, 1354440. https://doi.org/10.3389/fmicb.2024.1354440

4. Yan, A.; Chen, Z. Impacts of silver nanoparticles on plants: A focus on the phytotoxicity and underlying mechanism. *Int. J. Mol. Sci.* **2019**, 20, 1003. https://doi.org/10.3390/ijms20051003

5. Khan, S.; Zahoor, M.; Sher Khan, R.; Ikram, M.; Islam, N. U. The impact of silver nanoparticles on the growth of plants: The agriculture applications. *Heliyon* **2023**, *9*, 16928. https://doi.org/10.1016/j.heliyon.2023.e16928

6. Almutairi, Z.; Alharbi, A. Effect of silver nanoparticles on seed germination of crop plants. *J. Adv. Agric.* **2015**, *4*, 280–285. https://doi.org/10.24297/jaa.v4i1.4295

7. Noori, A.; Hasanuzzaman, M.; Roychowdhury, R.; Sarraf, M.; Afzal, S.; Das, S.; Rastogi, A. Silver nanoparticles in plant health: Physiological response to phytotoxicity and oxidative stress. *Plant Physiol. Biochem.* **2024**, *209*, 108538. https://doi.org/10.1016/j.plaphy.2024.108538

8. Guzmán-Báez, G. A.; Trejo-Téllez, L. I.; Ramírez-Olvera, S. M.; Salinas-Ruíz, J.; Bello-Bello, J. J.; Alcántar-González, G.; Hidalgo-Contreras, J. V.; Gómez-Merino, F. C. Silver nanoparticles increase nitrogen, phosphorus, and potassium concentrations in leaves and stimulate root length and number of roots in tomato seedlings in a hormetic manner. *Dose-Response Publ. Int. Hormesis. Soc.* **2021**, *19*, 15593258211044576. https://doi.org/10.1177/15593258211044576

9. Iqbal, M.; Raja, N. I.; Mashwani, Z-U. R.; Hussain, M.; Ejaz, M.; Yasmeen, F. Effect of silver nanoparticles on growth of wheat under heat stress. *Iran. J. Sci. Technol. Trans. Sci.* **2019**, *43*, 387–395. https://doi.org/10.1007/s40995-017-0417-4

10. Sadak, M. S. Impact of silver nanoparticles on plant growth, some biochemical aspects, and yield of fenugreek plant (*Trigonella foenum-graecum*). *Bull. Natl. Res. Cent.* **2019**, *43*, 38. https://doi.org/10.1186/s42269-019-0077-y

11. Vishwakarma, K.; Shweta; Upadhyay, N.; Singh, J.; Liu, S.; Singh, V. P.; Prasad, S. M.; Chauhan, D. K.; Tripathi, D. K.; Sharma, S. Differential phytotoxic impact of plant mediated silver nanoparticles (AgNPs) and silver nitrate ($AgNO_3$) on *Brassica* sp. *Front. Plant Sci.* **2017**, *8*, 1501. https://doi.org/10.3389/fpls.2017.01501

12. Yang, Y.; Xu, S.; Xu, G.; Liu, R.; Xu, A.; Chen, S.; Wu, L. Effects of ionic strength on physicochemical properties and toxicity of silver nanoparticles. *Sci. Total Environ.* **2019**, *647*, 1088–1096. https://doi.org/10.1016/j.scitotenv.2018.08.064

13. Sharma, P.; Chauhan, N. S. Effect on nanoparticles on plant cell morphology, physiology, and metabolism. In *The Impact of Nanoparticles on Agriculture and Soil*; Chauhan, N. S., Gill, S. S., Eds.; Academic Press: London, UK, 2023; pp. 95–113. https://doi.org/10.1016/B978-0-323-91703-2.00004-X

14. Angelini, J.; Klassen, R.; Široká, J.; Novák, O.; Záruba, K.; Siegel, J.; Novotná, Z.; Valentová, O. Silver nanoparticles alter microtubule arrangement, dynamics and stress phytohormone levels. *Plants* **2022**, *11*, 313. https://doi.org/10.3390/plants11030313

15. Zhang, H.; Zheng, T.; Wang, Y.; Li, T.; Chi, Q. Multifaceted impacts of nanoparticles on plant nutrient absorption and soil microbial communities. *Front. Plant Sci.* **2024**, *15*. https://doi.org/10.3389/fpls.2024.1497006

16. Xu, Y.; Chen, Z.; Li, X.; Tan, J.; Liu, F.; Wu, J. The mechanism of promoting rhizosphere nutrient turnover for arbuscular mycorrhizal fungi attributes to recruited functional bacterial assembly. *Mol. Ecol.* **2023**, *32*, 2335–2350. https://doi.org/10.1111/mec.16880

17. Wang, J.; Shu, K.; Zhang, L.; Si, Y. Effects of silver nanoparticles on soil microbial communities and bacterial nitrification in suburban vegetable soils. *Pedosphere* **2017**, *27*, 482–490. https://doi.org/10.1016/S1002-0160(17)60344-8

18. Plokhovska, S.; García-Villaraco, A.; Lucas, J. A., Gutierrez-Mañero, F. J.; Ramos-Solano, B. Silver nanoparticles coated with metabolites of *Pseudomonas* sp. N5.12 inhibit bacterial pathogens and fungal phytopathogens. *Sci. Rep.* **2025**, *15*, 1522. https://doi.org/10.1038/s41598-024-84503-z

19. Plokhovska, S.; Fuente-González, E.; Gutierrez-Albanchez, E.; Gutierrez-Mañero, F.-J.; Ramos-Solano, B. AgNPs biosynthesized from *Pseudomonas* Z9.3 metabolites as antimicrobial agents against bacterial and fungal pathogens. *Front. Microbiol.* **2025**, *16*, 1565689. https://doi.org/10.3389/fmicb.2025.1565689

20. Lucas, J. A.; Garcia-Villaraco, A.; Montero-Palmero, M. B.; Montalban, B.; Ramos-Solano, B.; Gutierrez-Mañero, F. J. Physiological and genetic modifications induced by Plant-Growth-Promoting Rhizobacteria (PGPR) in tomato plants under moderate water stress. *Biology* **2023**, *12*, 901. https://doi.org/10.3390/biology12070901

21. Martin-Rivilla, H.; Garcia-Villaraco, A.; Ramos-Solano, B.; Gutierrez-Mañero, F. J.; Lucas, J. A. Bioeffectors as biotechnological tools to boost plant innate immunity: signal transduction pathways involved. *Plants* **2020**, *9*, 1731. https://doi.org/10.3390/plants9121731

22. Thomas, K. M.; Spitzer, N. Silver nanoparticles induce formation of multi-protein aggregates that contain cadherin but do not colocalize with nanoparticles. *Toxicol. In Vitro* **2024**, *98*, 105837. https://doi.org/10.1016/j.tiv.2024.105837

23. Rani, S.; Kumari, N.; Sharma, V. Uptake, translocation, transformation and physiological effects of nanoparticles in plants. *Arch. Agron. Soil Sci.* **2023**, *69*, 1579–1599. https://doi.org/10.1080/03650340.2022.2103549

24. Wang, P.; Lombi, E.; Zhao, F-J.; Kopittke, P. M. Nanotechnology: A new opportunity in plant sciences. *Trends Plant Sci.* **2016**, *21*, 699–712. https://doi.org/10.1016/j.tplants.2016.04.005

25. Chen, S.; Yan, X.; Peralta-Videa, J. R.; Su, Z.; Hong, J.; Zhao, L. Biological effects of AgNPs on crop plants: environmental implications and agricultural applications. *Environ. Sci. Nano* **2023**, *10*, 62–71. https://doi.org/10.1039/D2EN00801G

26. Jiang, L.; Xiang, S.; Lv, X.; Wang, X.; Li, F.; Liu, W.; Liu, C.; Ran, M.; Huang, J.; Xu, X.; Ma, X.; Jin, Y.; Sun, X. Biosynthesized silver nanoparticles inhibit *Pseudomonas syringae* pv. *tabaci* by directly destroying bacteria and inducing plant resistance in *Nicotiana benthamiana*. *Phytopathol. Res.* **2022**, *4*, 43 (2022). https://doi.org/10.1186/s42483-022-00148-8

27. Bibi, S.; Raza, M.; Shahbaz, M.; Ajmal, M.; Mehak, A.; Fatima, N.; Abasi, F.; Sathiya Seelan, J.S.; Raja, N.I.; Yongchao, B.; Zain, M.; Javaid, R.A.; Maimaiti, Y. Biosynthesized silver nanoparticles enhanced wheat resistance to *Bipolaris sorokiniana*. *Plant Physiol. Biochem.* **2023**, *203*, 108067. https://doi.org/10.1016/j.plaphy.2023.108067

28. Goessling, J. W.; Yanyan, S.; Kühl, M.; Ellegaard, M. Frustule photonics and light harvesting strategies in diatoms. In *Diatom Morphogenesis*; John Wiley & Sons, Ltd: Hoboken, NJ, USA, 2021; pp. 269–300. https://doi.org/10.1002/9781119488170.ch12

29. Alabdallah, N. M.; Hasan, Md. M. Plant-based green synthesis of silver nanoparticles and its effective role in abiotic stress tolerance in crop plants. *Saudi J. Biol. Sci.* **2021**, *28*, 5631–5639. https://doi.org/10.1016/j.sjbs.2021.05.081

30. Ansari, M.; Ahmed, S.; Abbasi, A.; Hamad, N. A.; Ali, H. M.; Khan, M. T.; Haq, I. U.; Zaman, Q. Green synthesized silver nanoparticles: A novel approach for the enhanced growth and yield of tomato against early blight disease. *Microorganisms* **2023**, *11*, 886. https://doi.org/10.3390/microorganisms11040886

31. Morales, M.; Munné-Bosch, S. Malondialdehyde: Facts and Artifacts. *Plant Physiol.* **2019**, *180*, 1246–1250. https://doi.org/10.1104/pp.19.00405

32. Yonathan, K.; Mann, R.; Mahbub, K. R.; Gunawan, C. The impact of silver nanoparticles on microbial communities and antibiotic resistance determinants in the environment. *Environ. Pollut.* **2022**, *293*, 118506. https://doi.org/10.1016/j.envpol.2021.118506

33. Kalwani, M.; Chakdar, H.; Srivastava, A.; Pabbi, S.; Shukla, P. Effects of nanofertilizers on soil and plant-associated microbial communities: Emerging trends and perspectives. *Chemosphere* **2022**, *287*, 132107. https://doi.org/10.1016/j.chemosphere.2021.132107

34. Gray, D. B.; Gagnon, V.; Button, M.; Farooq, A. J.; Patch, D. J.; Wallace, S. J.; Koch, I.; O'Carroll, D. M.; Weber, K. P. Silver nanomaterials released from commercial textiles have minimal impacts on soil microbial

communities at environmentally relevant concentrations. *Sci. Total Environ.* **2022**, *806*, 151248. https://doi.org/10.1016/j.scitotenv.2021.151248

35. Zhai, Y.; Hunting, E.; Wouters, M.; Peijnenburg, W.; Vijver, M. Silver nanoparticles, ions, and shape governing soil microbial functional diversity: Nano shapes micro. *Front. Microbiol.* **2016**, *7*, 1–9. https://doi.org/10.3389/fmicb.2016.01123

36. McGee, C. F.; Storey, S.; Clipson, N.; Doyle, E. Soil microbial community responses to contamination with silver, aluminium oxide and silicon dioxide nanoparticles. *Ecotoxicology* **2017**, *26*, 449–458. https://doi.org/10.1007/s10646-017-1776-5

37. Bulgarelli, D.; Schlaeppi, K.; Spaepen, S.; Themaat, E. V. L. van; Schulze-Lefert, P. Structure and functions of the bacterial microbiota of plants. *Annu. Rev. Plant Biol.* **2013**, *64*, 807–838. https://doi.org/10.1146/annurev-arplant-050312-120106

38. Vuolo, F.; Novello, G.; Bona, E.; Gorrasi, S.; Gamalero, E. Impact of plant-beneficial bacterial inocula on the resident bacteriome: Current knowledge and future perspectives. *Microorganisms* **2022**, *10*, 2462. https://doi.org/10.3390/microorganisms10122462

39. Peiffer, J. A.; Spor, A.; Koren, O.; Jin, Z.; Tringe, S. G.; Dangl, J. L.; Buckler, E. S.; Ley, R. E. Diversity and heritability of the maize rhizosphere microbiome under field conditions. *Proc. Natl. Acad. Sci.* **2013**, *110*, 6548–6553. https://doi.org/10.1073/pnas.1302837110

40. Porra, R. J.; Thompson, W. A.; Kriedemann, P. E. Determination of accurate extinction coefficients and simultaneous equations for assaying chlorophylls *a* and *b* extracted with four different solvents: verification of the concentration of chlorophyll standards by atomic absorption spectroscopy. *Biochim. Biophys. Acta BBA - Bioenerg.* **1989**, *975*, 384–394. https://doi.org/10.1016/S0005-2728(89)80347-0

41. Lichtenthaler, H. Chlorophylls and carotenoids: Pigments of photosynthetic biomembranes. *Methods Enzymol.* **1987**, *148C*, 350–382. https://doi.org/10.1016/0076-6879(87)48036-1

42. Shukla, V.; Kumar, S.; Tripathi, Y. N.; Upadhyay, R. S. *Bacillus subtilis-* and *Pseudomonas fluorescens-*mediated systemic resistance in tomato against sclerotium rolfsii and study of physio-chemical alterations. *Front. Fungal Biol.* **2022**, *3*. https://doi.org/10.3389/ffunb.2022. 851002

43. Hu, Z.; Fan, J.; Chen, K.; Amombo, E.; Chen, L.; Fu, J. Effects of ethylene on photosystem II and antioxidant enzyme activity in *Bermuda grass* under low temperature. *Photosynth. Res.* **2016**, *128*, 59–72. https://doi.org/10.1007/s11120-015-0199-5

44. García-Limones, C.; Hervás, A.; Navas-Cortés, J. A.; Jiménez-Díaz, R. M.; Tena, M. Induction of an antioxidant enzyme system and other oxidative stress markers associated with compatible and incompatible interactions between chickpea (*Cicer arietinum* L.) and *Fusarium oxysporum* f. sp.*ciceris*. *Physiol. Mol. Plant Pathol.* **2002**, *61*, 325–337. https://doi.org/10.1006/pmpp.2003.0445

45. Xu, B. J.; Chang, S. K. C. A comparative study on phenolic profiles and antioxidant activities of legumes as affected by extraction solvents. *J. Food Sci.* **2007**, *72*, S159-166 (2007). https://doi.org/10.1111/j.1750-3841.2006.00260.x

46. Garland, J. L.; Mills, A. L. Classification and characterization of heterotrophic microbial communities on the basis of patterns of community-level sole-carbon-source utilization. *Appl. Environ. Microbiol.* **1991**, *57*, 2351–2359. https://doi.org/10.1128/aem.57.8.2351-2359.1991

47. Shannon, C.E.; Weaver, W. *The Mathematical Theory of Communication*; University of Illinois Press: Urbana, IL, USA, 1963.

48. Parada, A. E.; Needham, D. M.; Fuhrman, J. A. Every base matters: assessing small subunit rRNA primers for marine microbiomes with mock communities, time series and global field samples. *Environ. Microbiol.* **2016**, *18*, 1403–1414. https://doi.org/10.1111/1462-2920.13023

49. Quince, C.; Lanzen, A.; Davenport, R. J.; Turnbaugh, P. J. Removing noise from pyrosequenced amplicons. *BMC Bioinformatics* **2011**, *12*, 38. https://doi.org/10.1186/1471-2105-12-38

50. Gardes, M.; Bruns, T. D. ITS primers with enhanced specificity for basidiomycetes - application to the identification of mycorrhizae and rusts. *Mol. Ecol.* **1993**, *2*, 113–118. https://doi.org/10.1111/j.1365-294x.1993.tb00005.x

51. White, T. J.; Bruns, T.; Lee, S.; Taylor, J. Amplification and direct sequencing of fungal ribosomal RNA genes for phylogenetics. In *PCR Protocols*; Innis, M. A.; Gelfand, D. H.; Sninsky, J. J.; White, T. J., Eds.;

Academic Press: San Diego, CA, USA, 1990; pp. 315–322. https://doi.org/10.1016/B978-0-12-372180-8.50042-1

52. Hung, Y.-M.; Lu, T.-P.; Tsai, M.-H.; Lai, L.-C.; Chuang, E. Y. EasyMAP: A user-friendly online platform for analyzing 16S ribosomal DNA sequencing data. *New Biotechnol.* **2021**, *63*, 37–44. https://doi.org/10.1016/j.nbt.2021.03.001

53. Rognes, T.; Flouri, T.; Nichols, B.; Quince, C.; Mahé, F. VSEARCH: a versatile open source tool for metagenomics. *PeerJ* **2016**, *4*, 2584. https://doi.org/10.7717/peerj.2584

54. Abarenkov, K.; Zirk, A.; Piirmann, T.; Pöhönen, R.; Ivanov, F.; Nilsson, R.H.; Kõljalg, U. UNITE QIIME release for Fungi. 2020. https://doi.org/10.15156/BIO/786385

55. Bokulich, N. A.; Kaehler, B. D.; Rideout, J. R.; Dillon, M.; Bolyen, E.; Knight, R.; Huttley, G. A.; Caporaso, J. G. Optimizing taxonomic classification of marker-gene amplicon sequences with QIIME 2's q2-feature-classifier plugin. *Microbiome* **2018**, *6*, 90. https://doi.org/10.1186/s40168-018-0470-z